THE STRONGEST EVIDENCE ONLY

A Consolidated, Illustrated Critical Assessment of the Shroud of Turin and the Sudarium of Oviedo

Converging the strongest physical, microscopic, chemical, forensic, historical, and comparative evidence — while excluding weaker claims.

CORE METHOD

Only claims with high directness, material relevance, and discriminatory value are retained. Speculative image-formation mechanisms, pollen geography, flower or coin images, exact submicrometer image-depth numbers, AB typing as individual identification, unvalidated large point-count matches, and claims that the 1988 radiocarbon result has been conclusively overturned are excluded from the core case.

Otangelo Grasso

Independent Researcher · Aracaju, SE, Brazil · 2026

Abstract

This consolidated assessment deliberately retains only the strongest evidence from the two source manuscripts and integrates the new textile and fiber-level explanatory material. The core case rests on eight evidentiary domains: the absence of a conventional pigment-and-binder body image; extreme microscopic superficiality without ordinary capillary penetration; analytical separation of the body image from known scorch and other cloth records; a genuine blood-derived wound record materially distinct from the body image; evidence that blood preceded the body-image alteration; an anatomically integrated crucifixion-trauma ensemble; pre-Lirey documentary evidence for an image-bearing burial shroud tradition; and the independently preserved, image-free physiological record of the Sudarium of Oviedo. The evidentiary force is conjunctive rather than numerical: an adequate origin model must satisfy all of these constraints together.

Keywords: Shroud of Turin; Sudarium of Oviedo; STURP; microscopy; image chemistry; bloodstain evidence; crucifixion; textile archaeology; authenticity

1. Evidentiary framework and chronological counterweight

1.1 Inclusion and exclusion rule

A claim is retained only when it is directly observable or instrumentally measured, strongly relevant to the origin of the object, and sufficiently discriminatory to constrain ordinary painting, dyeing, liquid transfer, simple thermal methods, or conventional artistic simulation. The purpose is not to count anomalies but to preserve the smallest set of observations that remains robust when weaker arguments are removed.

Claims dependent mainly on pollen geography, flower or coin images, disputed inscriptions, DNA identity, AB blood typing as individualization, unvalidated large same-person point counts, exact submicrometer image-depth numbers, exact VP-8 body-distance claims, speculative radiation/corona mechanisms, numerical forgery probabilities, or assertions that the 1988 radiocarbon result has already been conclusively overturned are excluded from the core case.

1.2 Chronological counterweight

IMPORTANT COUNTERWEIGHT

The 1988 AMS radiocarbon test remains the strongest direct chronological counterevidence. The tested corner sample yielded a calibrated medieval range of AD 1260–1390 [19]. This consolidated paper does not treat that result as scientifically refuted. The question addressed here is whether the strongest non-radiocarbon physical, forensic, and historical observations impose additional constraints that any complete origin hypothesis must explain.

1.3 Distribution of the retained evidence

The critical screening process retained 31 individual evidentiary observations distributed across eight domains. For clarity and to avoid double-counting closely related observations, the present paper does not discuss all 31 as separate arguments. Instead, correlated findings are consolidated into a smaller number of high-value evidentiary conclusions developed in Section 2.

The distribution below is descriptive rather than statistical. The number of observations in a category does not determine its evidentiary weight: a domain containing fewer strongly discriminatory findings may contribute more to the overall assessment than a domain containing several mutually dependent observations. The strength of the case therefore derives from convergence across substantially independent domains of measurement and analysis, not from the raw count of favorable claims.

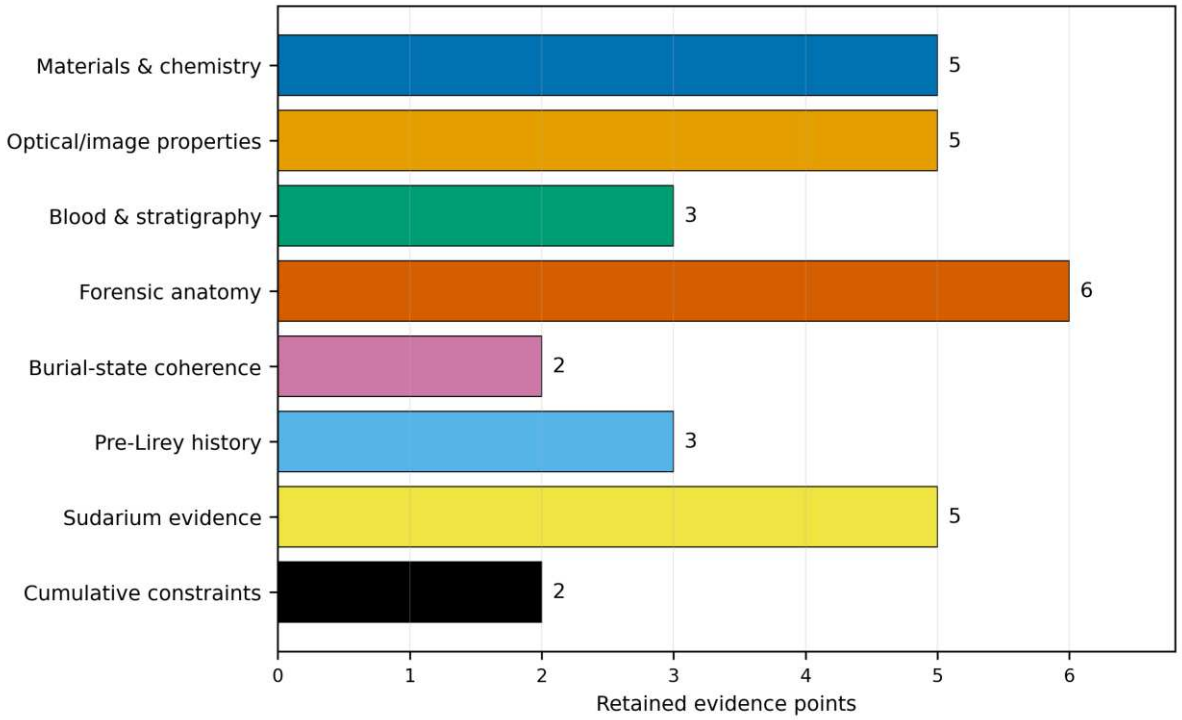


Figure 1. Distribution of the 31 retained evidentiary observations across eight domains. The chart is descriptive rather than a statistical weighting scheme: the number of observations in a domain does not determine its evidentiary weight.

Table 1. Evidentiary architecture of the retained set.

Domain	Points	Primary authenticity value	Principal restraint
Materials & chemistry	**5**	Constrains ordinary paint, binder, liquid, and bulk-coloration models.	Mechanism unresolved.
Optical/image properties	**5**	Independent spectral and geometric constraints on ordinary artistry.	Some formation inferences are model-dependent.
Blood & stratigraphy	**3**	Separate biological record plus a proposed temporal sequence.	Blood-before-image needs modern replication.
Forensic anatomy	**6**	Coherent crucifixion trauma; several details depart from medieval convention.	Specific flow mechanisms remain debated.
Burial-state coherence	**2**	Fits brief contact after violent death.	Supportive, not diagnostic.
Pre-Lirey history	**3**	Complicates a wholly novel 1350s French invention.	No continuous chain of custody.
Sudarium evidence	**5**	Independent bloodstained comparator preserved separately from the Shroud.	Same-person identification not validated.
Cumulative constraints	**2**	One model must satisfy the full conjunction, not isolated properties.	Future replication could change the balance.

2. The strongest consolidated evidentiary findings

The 31 screened observations are consolidated below into the strongest evidentiary findings. Closely related measurements are treated together rather than counted as independent arguments. Each section distinguishes the empirical observation from its explanatory significance and states the principal limitation where necessary.

Table 2. Consolidated evidentiary domains used in the present assessment.

Retained domain	Why it matters	Principal restraint
Image chemistry	No conventional pigment-and-binder system accounts for the body image.	Constrains ordinary painting; does not prove no artificial process.
Microscopic superficiality	Selected exposed fiber surfaces are altered while protected interiors remain largely uncolored.	Exact nanometer depth is not treated as established.
Spectral/record separation	UV, reflectance, microscopy, chemistry, and XRF distinguish image, blood, scorch, and linen.	Methods share one artifact; interpretations remain bounded.
Blood chemistry	Wound stains contain blood-derived constituents and form a separate material record.	Species/AB typing is unnecessary and excluded.
Blood-before-image sequence	Reduced image coloration beneath blood/serum implies deposition before later image alteration.	Needs modern independent replication at finer scale.
Crucifixion forensics	Multiple injury classes form one coherent trauma ensemble.	Specific trajectories and flow mechanisms remain debated.
Pre-Lirey documentary history	Robert de Clari records a figure-bearing burial shroud in Constantinople before Lirey.	Does not prove identity with the Turin cloth.
Sudarium physiology	Independent image-free blood/fluid cloth provides an external head-trauma comparator.	Same-person identification is not established.

3. Strongest evidence 1 — the body image is not an ordinary painting

Finding: no image-forming concentration of conventional pigment or binder was demonstrated in the body image, and the visible chromophore is principally an alteration of the linen itself. [1–4]

X-ray fluorescence did not reveal image-correlated distributions of iron, mercury, lead, or other heavy elements at concentrations capable of accounting for the body image. Protein-sensitive testing detected protein where expected in blood areas but did not demonstrate an image-forming protein binder in body-image fibers. STURP therefore interpreted the pale yellow-brown body image primarily as a chemical alteration of the linen carbohydrate structure rather than as a conventional colored layer deposited on the cloth. The strongest conclusion is narrow but important: the simplest medieval pigment-and-binder painting model is not supported.

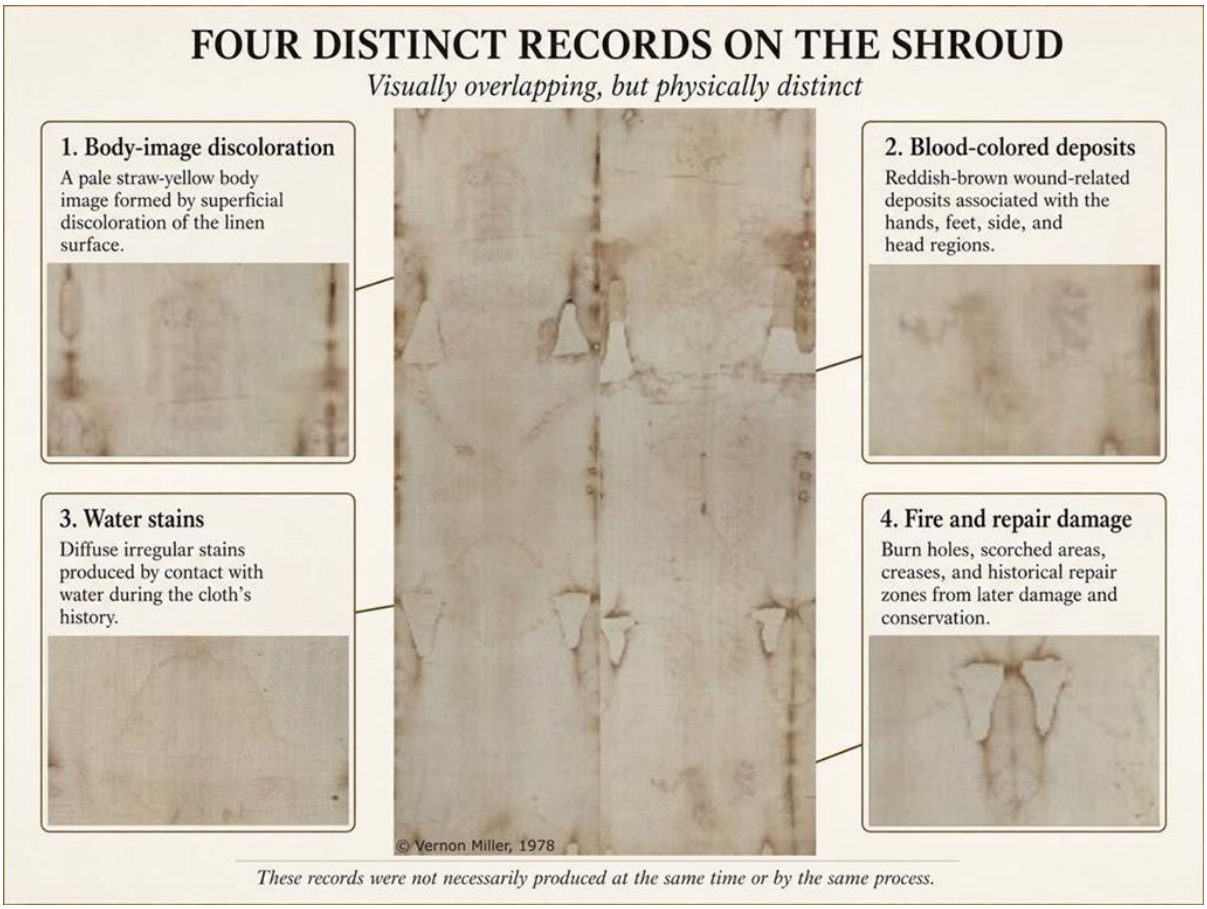


Figure 2. Four physically distinct records on the Shroud. Body-image discoloration, blood-colored deposits, water stains, and fire/repair damage overlap visually but are not one material system; spectroscopy, microscopy, chemistry, and UV imaging distinguish them.

4. Strongest evidence 2 — extreme microscopic superficiality and absence of liquid penetration

Finding: body-image coloration is concentrated on exposed surfaces of selected linen fibers and threads, while protected interior fibers remain substantially uncolored; the image lacks the wicking expected from an image-forming liquid. [1,4]

A linen thread is a bundle of many elementary flax fibers twisted together. Each elementary fiber is itself a plant cell with a layered wall surrounding a lumen. The important observation is not a disputed exact depth in nanometers: it is the selective location of the image alteration. Exposed fiber surfaces can carry the yellow-brown discoloration while many fibers protected within the thread remain comparatively uncolored. This is a severe constraint on ordinary liquid-based manufacture because absorbent linen normally draws fluids inward by capillary action, producing penetration, migration, pooling, or coloration deeper within the yarn.

The fiber-level distribution also helps explain the image's macroscopic tonality. Image density can vary through the proportion and distribution of colored versus uncolored microscopic fibers rather than through a thick, continuously applied paint layer. Any proposed formation mechanism must therefore account for selective surface alteration across a life-size image while preserving largely unaffected thread interiors.

FIGURE CAUTION

The following plate is a didactic microstructural reconstruction, not an original Shroud micrograph. Its purpose is to visualize the hierarchy from thread bundle to elementary flax fiber and the reported surface-selective distribution. Exact numerical image-depth values shown in the artwork are not used as retained evidence in this paper.

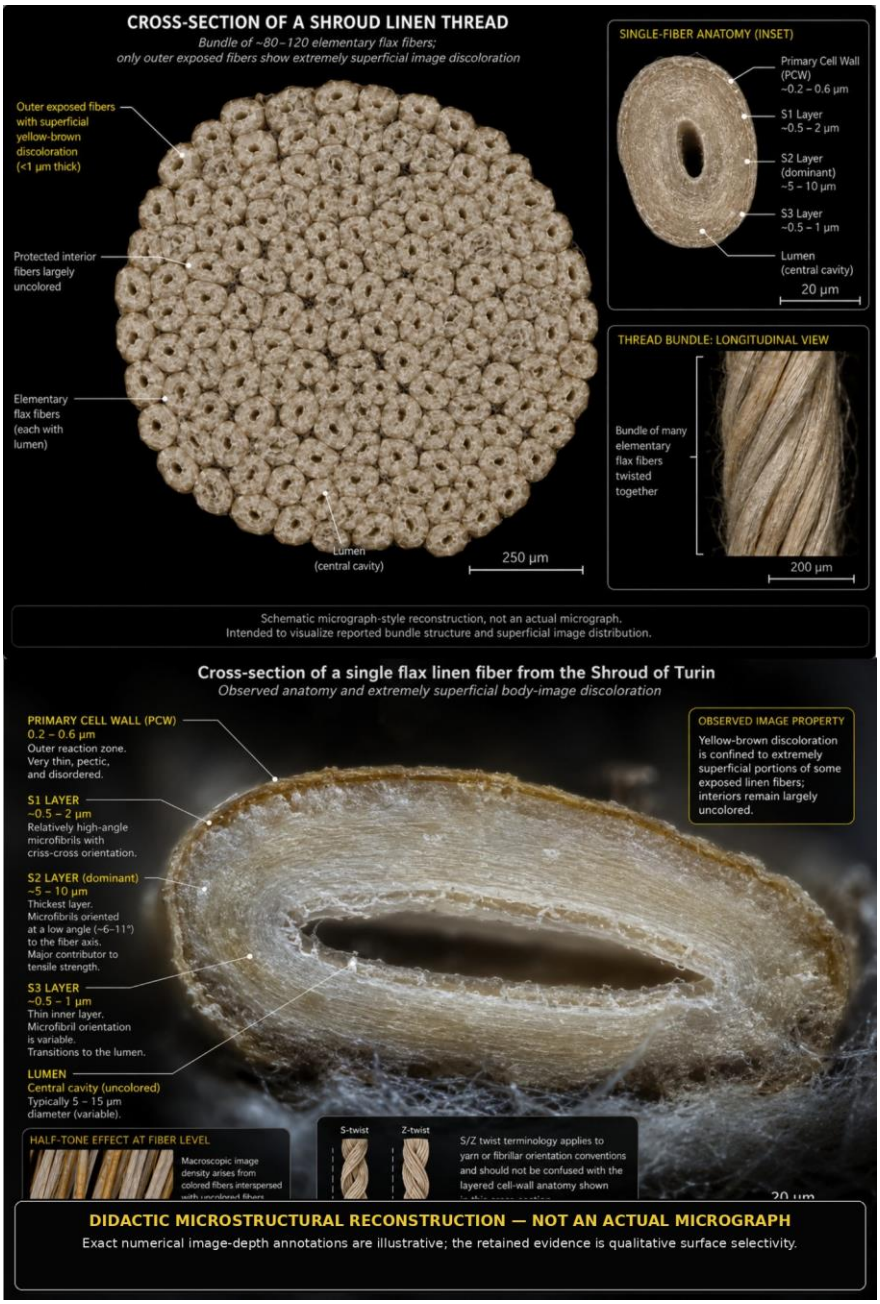


Figure 3. Didactic reconstruction of a linen thread bundle and an individual flax fiber. The retained evidentiary point is qualitative surface selectivity: some exposed fiber surfaces are discolored while protected interior fibers remain largely uncolored. Numerical depth annotations are illustrative and are not treated here as established measurements.

5. Strongest evidence 3 — the body image is analytically distinct from known scorch and other records

Finding: the body image and the documented 1532 fire scorches behave differently under ultraviolet examination, while independent analytical methods also separate image, blood, linen, and scorch. [1–7]

The Shroud contains its own internal control: unquestionably heat-damaged regions from the historical fire. Under ultraviolet excitation, those scorched regions display a characteristic fluorescence response, whereas body-image regions behave differently and largely quench the linen's native fluorescence rather than reproducing the scorch response. Reflectance spectroscopy, UV fluorescence, microscopy, chemistry, and X-ray fluorescence likewise discriminate the principal classes of markings. This substantially weakens simple heated-relief or ordinary scorching explanations without claiming that every conceivable thermal variant has been excluded.

WHY THIS IS STRONG

The value is methodological convergence. Different physical measurement principles independently distinguish the same records. The conclusion therefore does not rest on one photograph or one instrument.

6. Strongest evidence 4 — genuine blood-derived material forms a second marking system

Finding: wound-associated stains contain blood-derived chemical constituents and are materially different from the pale body image. [3,4,8]

Chemical testing of wound areas reported heme derivatives, proteins, and serum-associated material. The wound stains therefore constitute a materially distinct biological record rather than simply a red-painted component of the body image. The two systems are coordinated anatomically: blood-derived deposits occur in regions associated with the head, wrist/carpal area, side, feet, and the extensively scourged body. A deliberate-manufacture model must consequently explain both an unusual non-pigment body image and a separate biological wound record in correct registration.

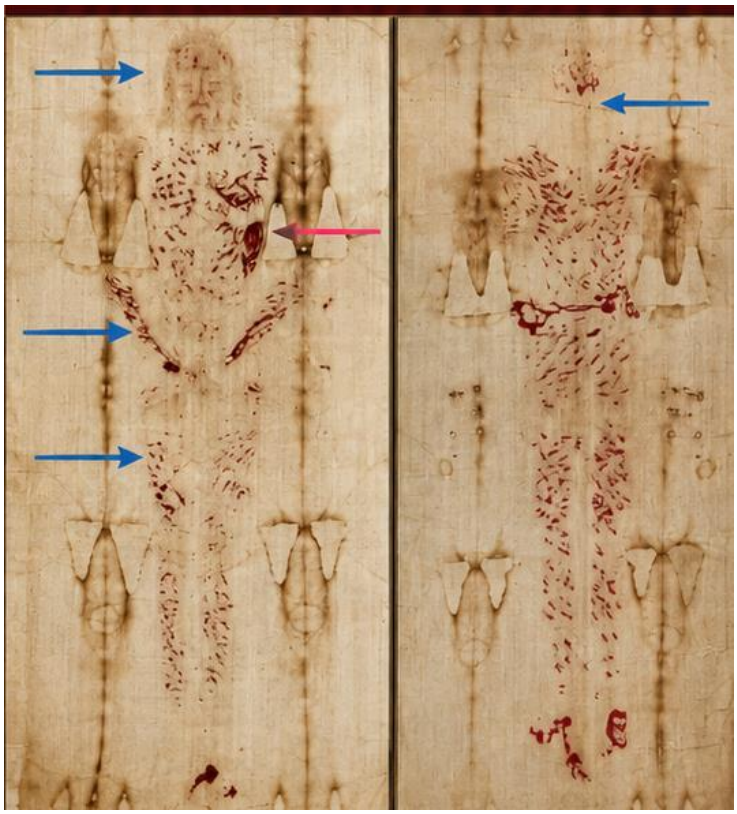


Figure 4. Anatomically distributed bloodstains on frontal and dorsal body regions. The plate visualizes the broad distribution of wound-associated stains; the conclusion that they contain blood-derived material rests on laboratory analyses rather than on color alone.

7. Strongest evidence 5 — blood preceded the body-image process

Finding: reduced body-image discoloration beneath blood-associated deposits indicates that blood/serum was already present before the later body-image alteration. [3,4]

STURP investigators reported that fibers protected beneath blood-associated deposits showed reduced image discoloration, leading to the inference that blood or serum masked the linen from the later image-forming process. If the cloth records contact with a wounded body, this sequence is natural: bleeding and deposition occur first, followed by whatever process later altered exposed linen surfaces. In an ordinary artistic workflow, by contrast, a maker would more intuitively construct the figure first and add wounds afterward. The result is therefore unusually discriminating, although modern independent replication of the micro-stratigraphy would strengthen it further.

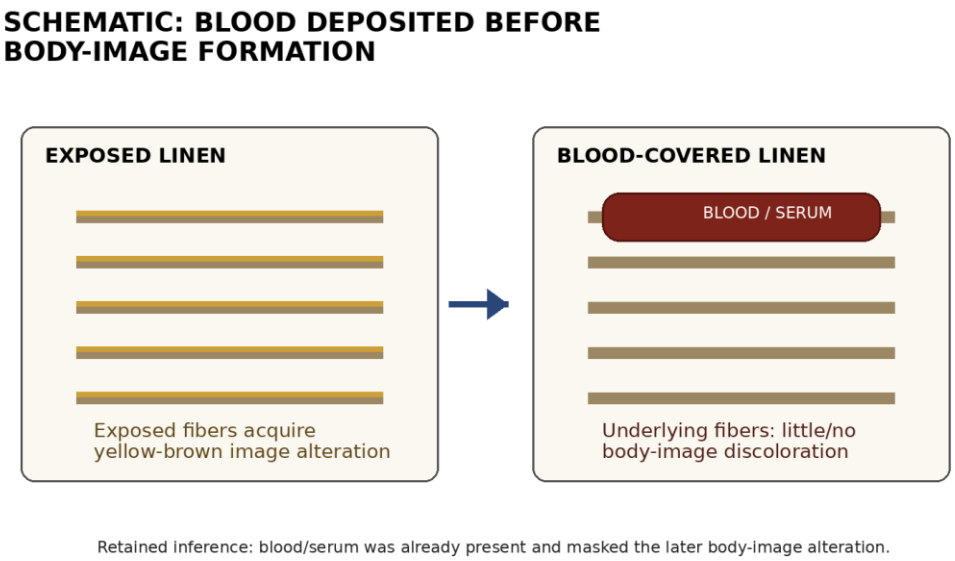


Figure 5. Blood-before-image stratigraphy. The schematic shows the reported masking relationship: exposed linen acquires pale body-image discoloration, whereas fibers protected beneath blood/serum deposits show reduced image coloration.

8. Strongest evidence 6 — a coherent crucifixion-trauma ensemble

Finding: the same individual bears wrist-region fixation wounds, extensive scourging, multiple scalp punctures, foot wounds, and a major side wound in one anatomically integrated pattern. [9–13]

The strongest forensic argument is not any isolated mark but the integration of multiple injury classes on one body. The principal upper-limb nail-associated pattern is localized to the wrist/carpal region rather than the center of the palm. Numerous scourge lesions are distributed across anterior and posterior surfaces; the scalp carries multiple puncture-associated blood flows rather than a single symbolic crown line; foot fixation and the major side wound complete the same trauma record. Several details depart from dominant medieval Crucifixion iconography in the direction of later anatomical plausibility. Exact nail trajectories, individual flow mechanisms, and the precise number of scourge blows are not required for the retained claim.

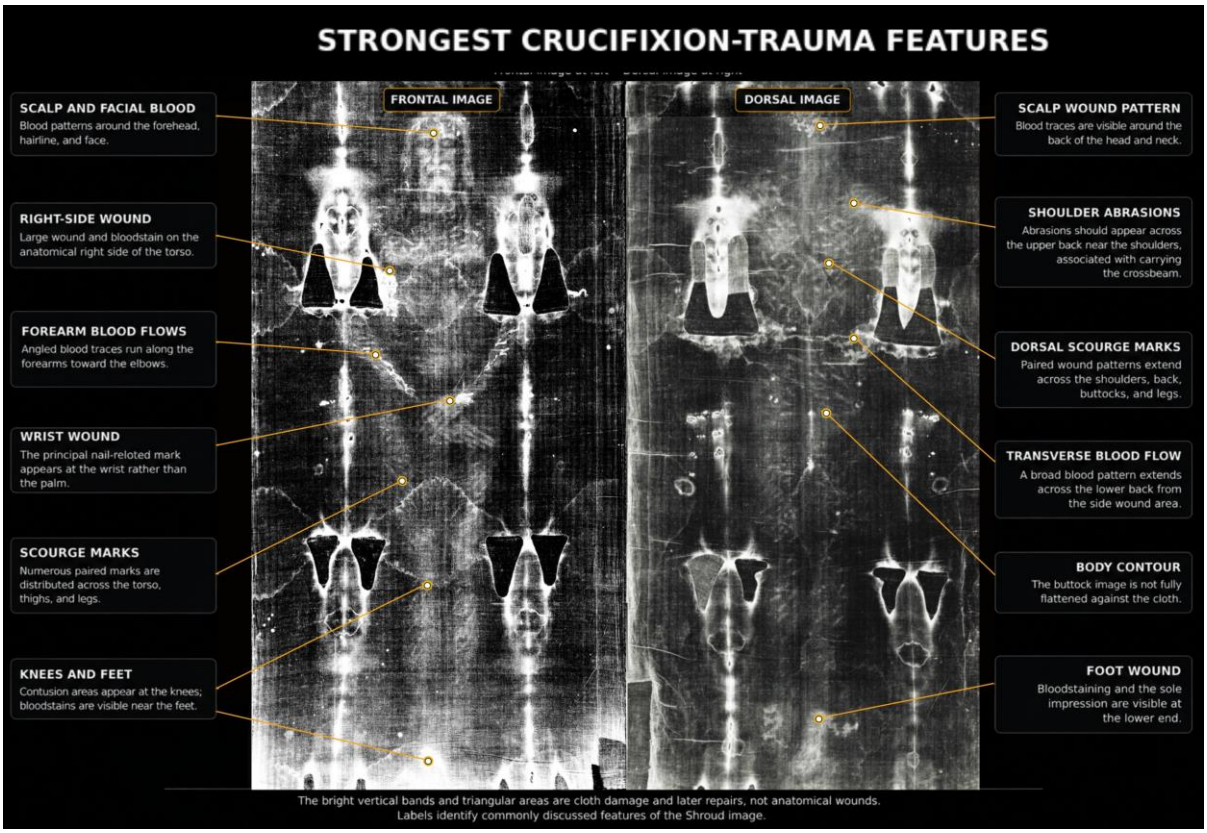


Figure 6. Five strongest crucifixion-trauma features: multiple scalp punctures, wrist-region fixation, widespread scourging, the major side wound, and foot fixation. Secondary and more debatable anatomical annotations are intentionally omitted.

9. Strongest evidence 7 — a pre-Lirey documentary witness

Finding: before the Shroud's secure appearance at Lirey, Robert de Clari described in Constantinople a burial shroud associated with Christ on which 'the figure of our Lord' could be seen. [14]

The Fourth Crusade chronicler Robert de Clari reported a sydoine at the Church of Blachernae in Constantinople in connection with Christ's burial and a visible figure. This does not establish an unbroken chain of custody to Turin and does not prove that the Constantinopolitan cloth was the same object. Its value is narrower: an image-bearing Christ burial-shroud tradition demonstrably existed roughly a century and a half before the Shroud's secure fourteenth-century French documentation. For that reason it complicates a hypothesis in which the entire concept first arose as a wholly novel invention at Lirey.

EXCLUDED FROM THIS CORE

The Pray Codex and other iconographic parallels are not needed here. They may be suggestive, but feature selection is more interpretive than the direct documentary statement of Robert de Clari.

10. Strongest evidence 8 — the Sudarium of Oviedo is an independent physiological comparator

Finding: the Sudarium is a separately preserved linen with concentrated blood/fluid staining but no body image; its stains are studied as a physiological record produced by contact, gravity, head position, and post-mortem handling. [15–18]

The Sudarium's evidentiary value lies primarily in independence. It does not reproduce the Shroud's body image and therefore cannot function as a simple visual copy. Instead, it preserves an image-free blood/fluid record associated with the head region and has an independent custodial history in Spain predating Lirey. Comparative studies report anatomically compatible cranial stain patterns between the two cloths. The strongest defensible formulation is not individual identification by AB typing or by an unvalidated large point count, but the existence of a separately preserved physiological head-trauma record that is mechanistically different yet anatomically compatible with the type of violently injured individual represented on the Shroud.

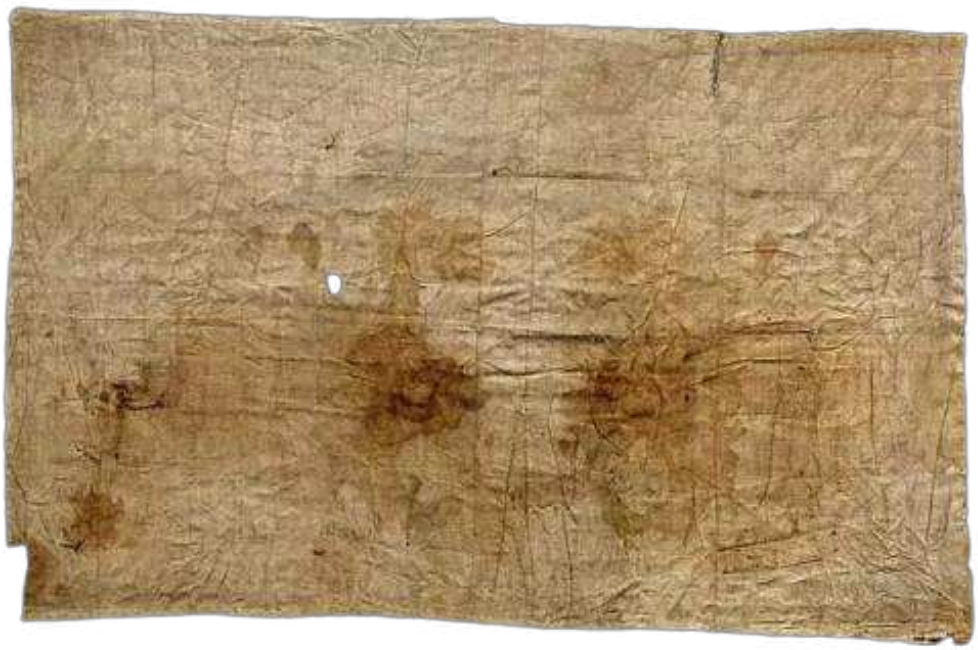


Figure 7. Sudarium of Oviedo — artifact view. Unlike the Shroud, the cloth bears no body image; its evidentiary content is the distribution of blood and other fluids on an independently preserved head cloth.

11. Textile context — why the linen is called a 3:1 herringbone twill

Contextual finding: the Shroud is woven in a 3:1 herringbone twill. This is a meaningful description of textile technology, but it is not used here as a dating proof. [1,20]

In the weave sequence illustrated below, a weft yarn passes over three warp yarns and then under one warp yarn; the sequence repeats. Successive rows are offset so that the interlacing develops a diagonal twill line. When the direction of that diagonal is periodically reversed, the surface forms the characteristic chevron or 'herringbone' pattern. Thus, '3:1' describes the repeating over-three/under-one interlacing, while 'herringbone' describes the periodic reversal of the twill direction.

Compared with ordinary plain or tabby linen, such a structure is more elaborate to set up and weave. It demands controlled multi-shed sequencing, consistent yarn preparation and tension, and deliberate reversal of the twill direction. A large, fine linen sheet of this type therefore represents more textile labor and skill than a simple coarse plain weave and would reasonably have been a higher-value cloth. However, the weave itself does not identify a specific century or place of origin: 3:1 twill was known before the Middle Ages, and the Shroud's textile structure should be treated as contextual evidence rather than a chronological test.

RARITY AND COST — CAREFUL FORMULATION

The safest statement is not that 3:1 herringbone linen was 'unknown' or uniquely rare. Rather, it was more technically demanding and less commonplace than simple plain weave, especially when executed as a large, fine, regular linen cloth. The inference of higher cost comes from the additional material preparation, loom setup, weaving control, and skilled labor required.

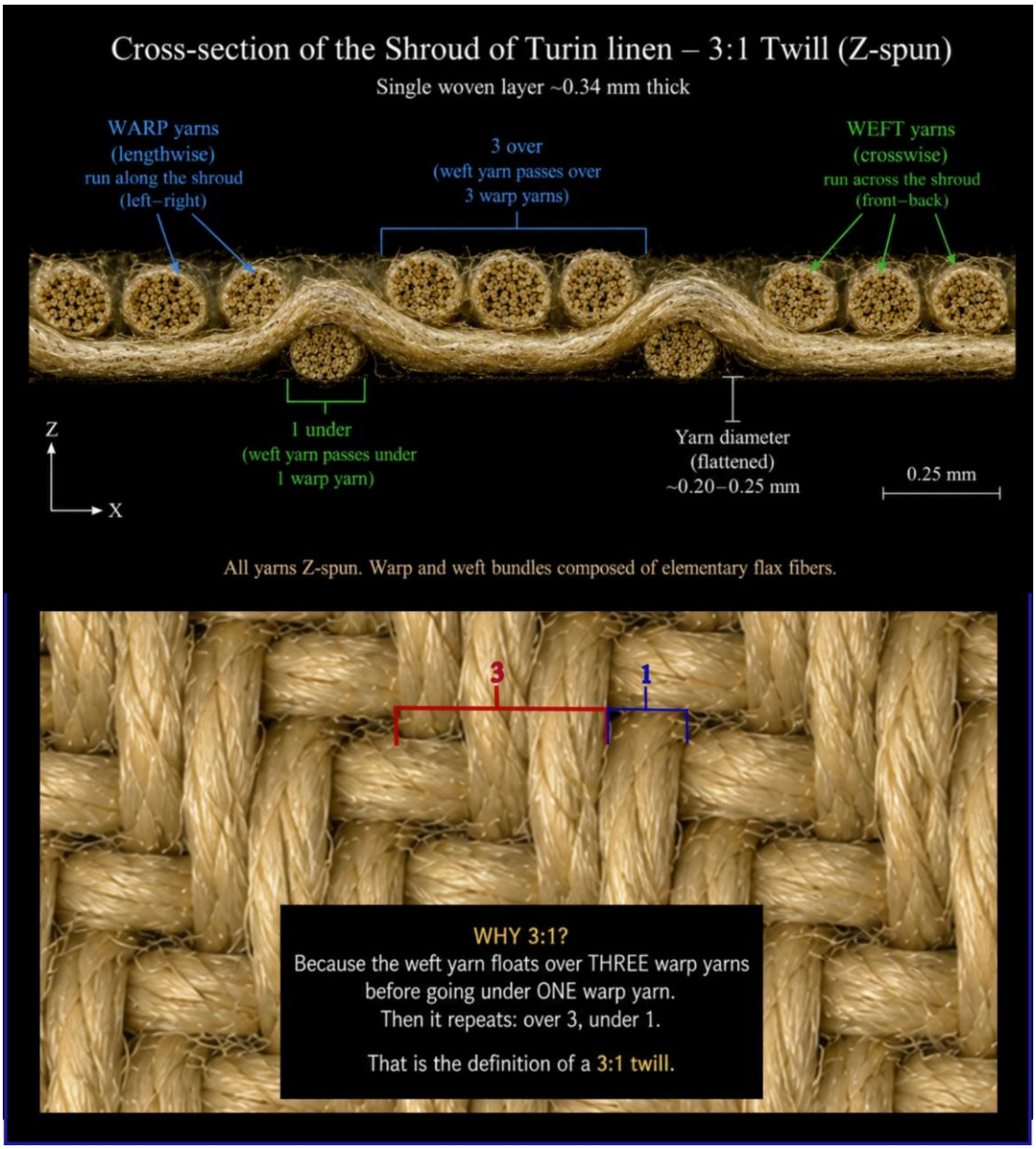


Figure 8. Enlarged top-down explanation of the 3:1 repeat. The tracked weft passes over three warp yarns, then under one, before the sequence repeats. The figure explains the terminology; it is not a dating test.

12. The cumulative constraint

One explanation must account for all retained properties together.

The strongest case is conjunctive. A proposed origin must simultaneously explain: (1) a life-size body image without a conventional pigment-and-binder system; (2) extreme surface selectivity without normal liquid wicking; (3) analytical behavior distinct from known scorch and other material records; (4) a separate biological blood record; (5) blood deposition before body-image formation; (6) an anatomically integrated crucifixion-trauma ensemble; (7) a pre-Lirey image-bearing burial-shroud documentary tradition; and (8) independent physiological corroboration from the Sudarium. The 3:1 herringbone weave adds textile context but is intentionally not counted as an independent authenticity proof.

Modern reconstructions have reproduced selected subsets of Shroud-like properties, but the two source manuscripts correctly emphasize that reproducing one yellow image, one wound pattern, one negative-like face, or one superficial effect is not equivalent to reproducing the complete integrated object. The explanatory burden lies in satisfying the full conjunction while also accounting for the 1988 radiocarbon result.

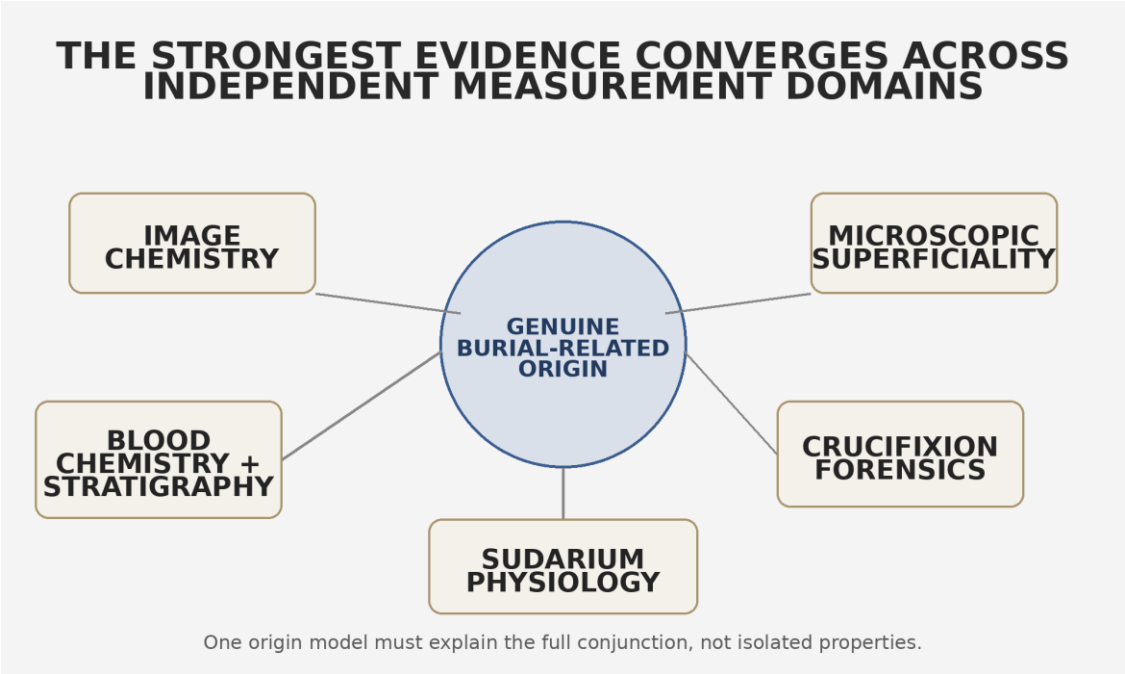


Figure 9. Architecture of the strongest cumulative case. The diagram is organizational rather than an additional line of evidence: chemistry, microscopic superficiality, blood chemistry and stratigraphy, crucifixion forensics, and Sudarium physiology converge from substantially different measurement domains.

13. Conclusion

After the weaker and more controversial arguments are removed, the evidentiary core remains substantial. The Shroud body image is materially unlike an ordinary pigment-and-binder painting, is concentrated on exposed linen surfaces without the bulk penetration expected from an image-forming liquid, and is analytically distinct from documented scorch and other cloth records. The wound system contains genuine blood-derived material and is physically separate from the body image; the reported stratigraphy indicates that blood was present before the later body-image alteration. The injuries form a coherent crucifixion-trauma pattern across the same individual. Robert de Clari provides a pre-Lirey documentary witness to an image-bearing burial shroud tradition, while the Sudarium of Oviedo contributes an independent, image-free physiological blood/fluid record from a severely injured head.

The new fiber-level and 3:1 herringbone plates improve explanation rather than inflate the evidence count. The fiber plate clarifies why microscopic surface selectivity is such a stringent physical constraint; the weave plate clarifies the technological meaning of 3:1 herringbone and why such linen represents skilled, comparatively costly manufacture while remaining non-diagnostic for date.

None of these observations individually identifies Jesus of Nazareth, and an unresolved image-formation mechanism is not itself evidence of a supernatural event. The central scientific question is comparative explanatory fit. A genuine burial-related origin naturally predicts a wounded body, biological deposits, integrated trauma, and burial-cloth behavior; a deliberate-manufacture hypothesis must reproduce the same chemistry, microscopy, stratigraphy, anatomy, historical context, and independent comparator while also explaining the medieval radiocarbon measurement. That unresolved tension is the proper target of future direct examination.

BOTTOM LINE

The case is stronger when it is narrower. Its force comes from the quality, independence, and convergence of the retained evidence — not from the raw number of favorable claims.

References

1. Schwalbe, L. A., & Rogers, R. N. (1982). Physics and chemistry of the Shroud of Turin: A summary of the 1978 investigation. Analytica Chimica Acta, 135, 3–49.

2. Morris, R. A., Schwalbe, L. A., & London, J. R. (1980). X-ray fluorescence investigation of the Shroud of Turin. X-Ray Spectrometry, 9(2), 40–47.

3. Heller, J. H., & Adler, A. D. (1981). A chemical investigation of the Shroud of Turin. Canadian Society of Forensic Science Journal, 14(3), 81–103.

4. Jumper, E. J., Adler, A. D., Jackson, J. P., Pellicori, S. F., Heller, J. H., & Druzik, J. R. (1984). A comprehensive examination of the various stains and images on the Shroud of Turin. Archaeological Chemistry III, ACS Advances in Chemistry Series 205, 447–476.

5. Gilbert, R., Jr., & Gilbert, M. M. (1980). Ultraviolet-visible reflectance and fluorescence spectra of the Shroud of Turin. Applied Optics, 19(12), 1930–1936.

6. Pellicori, S. F. (1980). Spectral properties of the Shroud of Turin. Applied Optics, 19(12), 1913–1920.

7. Miller, V. D., & Pellicori, S. F. (1981). Ultraviolet fluorescence photography of the Shroud of Turin. Journal of Biological Photography, 49(3), 71–85.

8. Heller, J. H., & Adler, A. D. (1980). Blood on the Shroud of Turin. Applied Optics, 19(16), 2742–2744.

9. Bucklin, R. (1982). The Shroud of Turin: A pathologist's viewpoint. Legal Medicine Annual, 1–11.

10. Zugibe, F. T. (2005). The Crucifixion of Jesus: A Forensic Inquiry. M. Evans & Co.

11. Edwards, W. D., Gabel, W. J., & Hosmer, F. E. (1986). On the physical death of Jesus Christ. JAMA, 255(11), 1455–1463.

12. Nicolotti, A. (2017). The scourge of Jesus and the Roman scourge: Historical and archaeological evidence. Journal for the Study of the Historical Jesus, 15(1), 1–32.

13. König, L., Schmölders, R., Jühling, M., et al. (2023). Some experiments and remarks regarding the possible formation of blood stains on the Turin Shroud. International Journal of Legal Medicine, 137, 863–878.

14. Robert de Clari. (c. 1216). La Conquête de Constantinople. Eyewitness chronicle of the Fourth Crusade and the relics of Constantinople.

15. Guscin, M. (1998). The Oviedo Cloth. Lutterworth Press.

16. Heras Moreno, G., Villalaín Blanco, J. D., & Rodríguez Almenar, J. M. (2015). Comparative Study of the Sudarium of Oviedo and the Shroud of Turin. Proceedings of the First International Congress on the Sudarium of Oviedo.

17. Hermosilla, A. S. (2015). Commonalities between the Shroud of Turin and the Sudarium of Oviedo. SHS Web of Conferences, 15.

18. Barta, C., et al. (2015). New coincidence between Shroud of Turin and Sudarium of Oviedo. SHS Web of Conferences, 15.

19. Damon, P. E., et al. (1989). Radiocarbon dating of the Shroud of Turin. Nature, 337, 611–615.

20. Vial, G. (1989). Le Linceul de Turin — Étude Technique. CIETA Bulletin, 67. Technical study of the Shroud textile and 3:1 herringbone structure.